Inorganic Chemistry

Article

pubs.acs.org/IC

Bonding and Structure of Oxofluoroniobate-Based Glasses

Natalia M. Laptash,* Irina G. Maslennikova, Arseny B. Slobodyuk, Valery Ya. Kavun, and Vladimir K. Goncharuk

Institute of Chemistry, Far Eastern Branch of Russian Academy of Sciences, 159 Pr. Stoletiya Vladivostoka, 690022 Vladivostok, Russia

Supporting Information

ABSTRACT: Glasses based on the oxofluoroniobate anion have been characterized by vibrational and solid-state NMR spectroscopy. The mechanism of glass formation in the systems K_2NbOF_5–MF_3 (M = Al, In) has been suggested. A glass network is built from the chains of corner-sharing octahedra through –Nb–F(O)–M– and –Nb–F–Nb– bridges. Isolated $NbOF_5^{2-}$ octahedra are also present, which is consistent with the glass composition. The high ionic mobility of $NbOF_5^{2-}$ due to its fast reorientations results in equalization of the Nb–O and Nb–F distances, which is reflected in the appearance of the IR band at 700–800 cm^{-1} not observed in the Raman spectrum. Its assignment to bridging –Nb–O–Nb– species accepted in the literature was not proven.

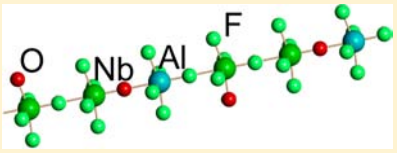

INTRODUCTION

Fluoride glasses have attracted substantial attention because of their intrinsic physical properties—high transparency and low phonon energy—which make them attractive materials for a number of photonic applications.[1] One of the attractive features of fluoride glasses lies in their predominant ionicity, making them a specific group of materials. The fluoride glass technology has outlined some common features, such as chemical reactivity of fluoride melts, devitrification tendency, and sensitivity to water. Most of the associated problems could be solved or partly controlled. In that sense, oxyfluoride glasses make a compromise between oxide and fluoride materials.[1]

An overview of oxyfluoride glasses was recently published,[2] but a critical estimation of the presented data was not made. The latter especially concerns the structure and bonding in glasses based on heavy-metal oxyfluorides, such as titanium, niobium, tantalum, molybdenum, and tungsten. Some physical properties of new oxyfluorovanadate glasses were reported.[3] Depending on the RF (RF = LiF, NaF) content in the V_2O_5–BaF_2–RF system, these property changes have been attributed to some structural ones: the creation of nonbridging fluorine ions.

The niobium oxyfluoride glasses have been extensively studied. The glass formation was initially examined in the K_2NbOF_5–AlF_3 system.[4] It was found that the glasses in this system were fast ionic conductors. The conductivity of the $0.74K_2NbOF_5$–$0.26AlF_3$ system was 1.045×10^{-2} $\Omega^{-1}\cdot cm^{-1}$. According to the Raman spectroscopy data, the $NbOF_5^{2-}$ anions were assumed to exist in an isolated octahedral structure and cannot connect with each other. On the other hand, the glasses obtained in the LiF–$BaNbOF_5$ and LiF–AlF_3–$BaNbOF_5$ systems were suggested to consist of disorderly packed corner-sharing or edge-sharing $NbOF_5^{2-}$ octahedra.[5]

Poulain et al.[6] assume that a vitreous network in the NbO_2F–BaF_2 system is built from the association of $Nb(O,F)_6$ polyhedra, the connectivity of which depends on the O/F and (O,F)/Nb ratios. It was suggested that octahedra must be isolated in the $40NbO_2F$–$60BaF_2$ binary glass: they could form chains or rings in the $50NbO_2F$–$50BaF_2$ phase. Unfortunately, no vibrational spectra were presented in this paper.

Ignat'eva and co-workers used vibrational spectroscopy and quantum-chemical calculations to characterize the glass structure based mainly on the starting oxofluoroniobates such as $CuNbOF_5\cdot 4H_2O$ and $MnNbOF_5\cdot 4H_2O$. Their numerous publications[7−16] evidence that the glass network is built from oxofluoroniobate polyhedra linked through oxygen bridges. However, the corresponding band is present in the IR spectrum but virtually absent in the Raman spectrum of the glasses. To clarify this peculiarity, syntheses in the glass-forming systems K_2NbOF_5–MF_3 (M = Al, In) were undertaken. The bonding and structure of synthesized glass materials were investigated by vibrational (IR and Raman) and NMR spectroscopy methods.

EXPERIMENTAL SECTION

Materials and Methods. The xK_2NbOF_5–$(1-x)MF_3$ (x = 0.75; M = Al, In) glasses were prepared by a conventional melt-quenching method using the reagent-grade MF_3 and single crystals of $K_2NbOF_5\cdot H_2O$. The latter were obtained from a fluoride solution of Nb_2O_5 with HF (40%), followed by the addition of KHF_2 or KCl in stoichiometric quantities. The resulting precipitate was dissolved in a HF solution with the addition of KF (20 g of precipitate and 4.5 g of KF). Transparent thin plates of $K_2NbOF_5\cdot nH_2O$ were crystallized under slow evaporation in air. Recrystallization of K_2NbF_7 from a hot aqueous solution led also to the same platelike $K_2NbOF_5\cdot nH_2O$ of triclinic syngony [see the Supporting Information (SI), Table S1]. Subsequent crystallizations in air gave monoclinic prismatic single crystals (Table S2 in the SI). The water content was dependent on the air humidity. At 50–70% humidity, thin plates that were used for glass preparation contained exactly one molecule of water, while at 15% humidity, the same crystals contained only $0.75H_2O$ (see the Figure S1 in the SI). Freshly prepared single crystals at 15% humidity contained 0.86- and $0.67H_2O$ for triclinic and monoclinic modifications,

Received: November 1, 2012
Published: April 30, 2013

   dx.doi.org/10.1021/ic302395x | Inorg. Chem. 2013, 52, 5722–5728

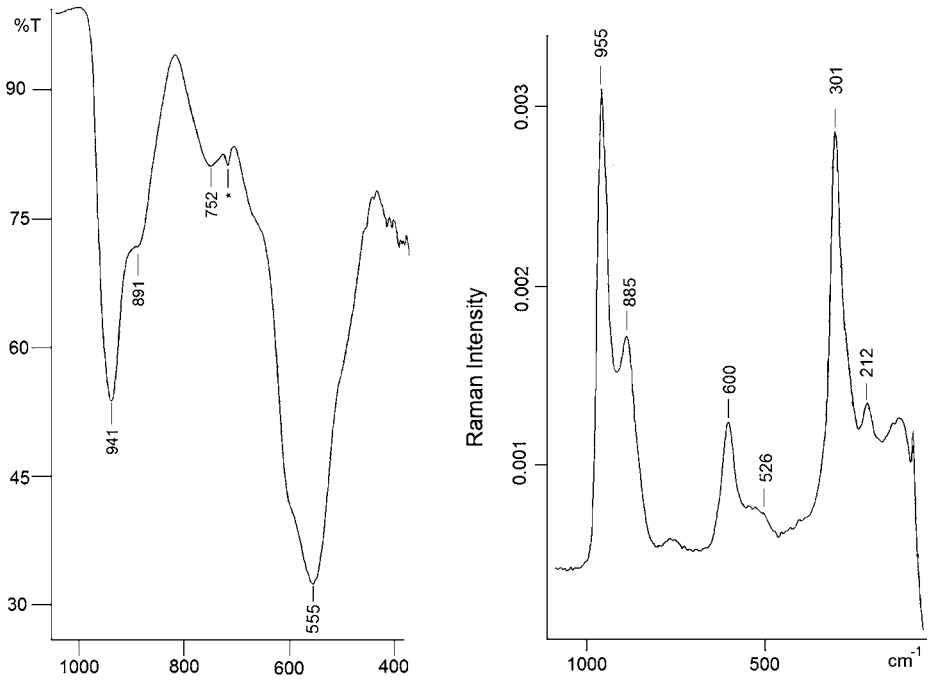

Figure 1. IR and Raman spectra of the $0.75K_2NbOF_5{-}0.25AlF_3$ glass. The asterisk designates the band of Nujol.

respectively. The water molecules were removed by heating the crystals at 350−400 °C for 20 min at an air humidity of 30%. No HF evolution was detected.

Freshly prepared anhydrous K_2NbOF_5 and powdered MF_3 (M = Al, In) were mixed, ground, and melted in a platinum crucible at 750 °C. The liquid melt was kept at this temperature for 10−15 min to ensure homogenization before it was cooled rapidly in a copper mold; transparent platelet glasses of a thickness of about 0.5 mm were obtained. X-ray diffraction (XRD) showed the samples to be amorphous.

$NaNbOF_4$, which was used as a reference compound with the chain structure, was prepared from Nb_2O_5 in a HF (40%) solution followed by the addition of NaF or NaCl at the molar ratio Na:Nb = 1:1. Transparent tetragonal prismatic single crystals were identified as monoclinic (Table S3 in the SI).

Mid-IR (400−4000 cm^{-1}) spectra of the glasses obtained were collected on the powdered glass sample in a Nujol mull using a Shimadzu FTIR Prestige-21 spectrometer operating at 2 cm^{-1} resolution. Raman spectroscopic measurements were conducted on a RFS 100/S spectrometer with a Nd:YAG laser at 1064 nm (130 mW output was used). All spectra were recorded at room temperature.

Solid-State NMR. The NMR spectra were measured on a Bruker AVANCE 300 spectrometer at Larmor frequency ν_L = 282.4 MHz (for ^{19}F nuclei, $I = {}^1/_2$) and 78.2 MHz (for ^{27}Al, $I = {}^5/_2$). The temperature adjustment accuracy was ±2 K. For static spectra, the one-pulse sequence was used. For magic-angle-spinning (MAS) spectra, both one-pulse and Hahn echo with a 90-τ-180 pulse, synchronized with the sample rotation period T ($\tau = nT$, n = 1−3), were employed. Isotropic signals were determined by comparing the spectra acquired with different spinning frequencies (from 10 to 18 kHz). The ^{19}F chemical shifts (CSs) were measured using C_6F_6 as a reference [$\delta(C_6F_6)$ versus $CFCl_3$ = −164.2 ppm], and the accuracy was 5 and 1 ppm for static and MAS spectra, respectively. An aqueous 1 M solution of aluminum nitrate was used as a reference for ^{27}Al CSs whose accuracy was ±1 ppm. The second-moment calculations of NMR spectra (S_2 in G^2) were carried out by the original program with the use of formulas presented elsewhere.[17]

RESULTS AND INTERPRETATION

Vibrational Spectroscopy Data. The glass composition of $0.75K_2NbOF_5{-}0.25AlF_3$ was chosen as intermediate in the glass-forming system $xK_2NbOF_5{-}(1{-}x)AlF_3$ (x = 0.69−0.79).[4] Its vibrational spectra (IR and Raman) are presented in Figure 1. Very strong bands in the range of 880−960 cm^{-1} are assigned to the Nb−terminal O stretching vibration. Normal coordinate analysis of isolated $NbOF_5^{2-}$ (C_{4v} symmetry) was made[18] and compared with experimental spectra of A_2NbOF_5 (A = Rb, Cs)[19] and $K_2NbOF_5{\cdot}H_2O$.[20] The range of 900−940 cm^{-1} is characteristic for ν_1 (A_1) Nb−O stretching vibration, which is both IR- and Raman-active. Such a frequency is in accordance with a short distance and the multiple (triple, one σ and two π) character of this bond.[21] Numerous crystal structure data of inorganic and hybrid compounds based on $NbOF_5^{2-}$ (where the O atom was localized) evidence the short Nb−O distance correlating to the corresponding strong high-frequency band (1.70−1.80 Å and 900−940 cm^{-1}, respectively).[22−32]

The shortest Nb−O distance (1.68 Å) reported was determined by electron diffraction for anhydrous K_2NbOF_5 without presenting its vibrational spectra.[33] The crystal structure of hydrated compound $K_2NbOF_5{\cdot}H_2O$ is not yet known precisely, but its IR and Raman spectra containing the split Nb−O stretch (at 943/926 and 939/925, respectively) are very similar to those of $(NH_4)_2NbOF_5$, which allows one to suppose two different independent states of the $NbOF_5$ octahedron in the crystal structure.[34] This feature is different, with the Nb−O stretches presented in Figure 1 containing at least two bands of some higher and lower frequencies relative to that of isolated $NbOF_5^{2-}$. The first one is assumed to be assigned to the Nb−O stretch with the O terminal atom (O_t) in the $NbOF_5^{2-}$ octahedron with bridging fluorines (F_b). The other one is, probably, related with the Nb−O−Al stretch. Very intensive bands at 500−600 cm^{-1} (maximum at 555 cm^{-1}) are assigned to Nb−F stretches in the $NbOF_5$ octahedron, and a shoulder at about 650 cm^{-1} is due to Al−F stretches in the AlF_6 octahedron.[35]

dx.doi.org/10.1021/ic302395x | Inorg. Chem. 2013, 52, 5722−5728

One should pay attention to a broad medium band in the IR spectrum of the sample glass at 700−800 cm^{-1} (Figure 1). Because this band overlaps partially with that of AlF_6, the vibrational spectra of the $0.75K_2NbOF_5$−$0.25InF_3$ glass were measured (Figure 2). Note that the discussed band is virtually

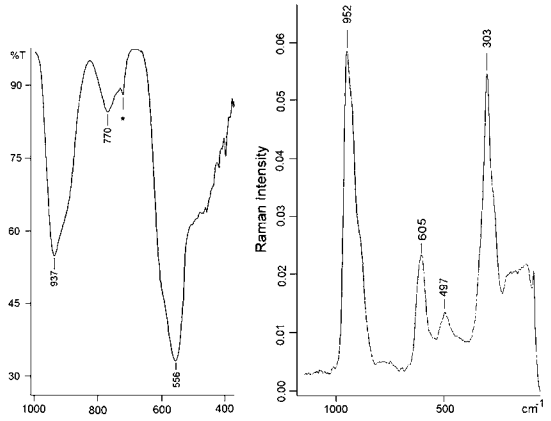

Figure 2. IR and Raman spectra of the $0.75K_2NbOF_5$−$0.25InF_3$ glass.

absent in the Raman spectra of the glass samples. Such a peculiarity is much more pronounced in the glasses based on $MnNbOF_5$ or $CuNbOF_5$,[10−16] where the intensities of the IR band at 700−800 cm^{-1} are comparable to or even higher than those of Nb−O stretches. The authors have assigned this band to bridging −Nb−O−Nb− vibrations. Indeed, the M−O−M stretches appear in the discussed range, but they are active and equally intensive in both IR and Raman spectra, as vibrational spectra of the chain structure $NaNbOF_4$ with bridging O atoms demonstrate (Figure 3).

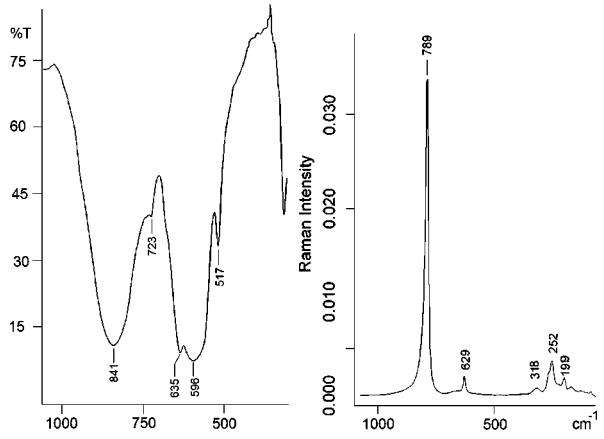

Figure 3. IR and Raman spectra of $NaNbOF_4$.

The $[NbOF_4]^-$ chains, built from *trans*-$[NbO_{2/2}F_4]$ octahedra, have been found in $ANbOF_4$ (A = NH_4 or alkali metal)[36] and hybrid $Ag(pyz)NbOF_4$.[37] These octahedra are bridged into a chain via their two *trans*-O atoms to yield alternately shorter (~1.8 Å) and longer Nb−O (~2.1 Å) bonds. Indeed, our density functional theory (DFT) calculations (B3LYP, 321G basis) of the $Nb_5O_4F_{22}^{5-}$ cluster show the −Nb−O−Nb− bridge to be asymmetrical. For less asymmetrical species, as in the case of $(NH_4)_2MoO_3F_2$ (short and long bonds are 1.880 and 2.007 Å, respectively),[38] the strong symmetrical and asymmetrical −Mo−O−Mo− vibrations lie at 655 and 673 cm^{-1}, respectively. For symmetrical species with O-*trans*-connected octahedra, as in the case of $(NH_4)_2TiOF_4$[39] (Ti−O 1.95 Å), these vibrations have virtually the same frequency (780 cm^{-1}).[40] In the layered structures of dioxodifluorovanadates AVO_2F_2 (A = Na, NH_4), both IR and Raman strong broad −V−O−V− stretches exhibit at 700−820 cm^{-1}.[41] Three-dimensional frameworks (3D network, ReO_3 type) of NbO_2F and TaO_2F oxyfluorides, consisting of corner-sharing $Nb(O,F)_6$ octahedra, are characterized by broad and very intensive bands in both their IR and Raman spectra at 600−800 cm^{-1}.[42,43] It turns out that locally the $Nb(O,F)_6$ octahedron is submitted to dynamically excited rigid unit mode rotations.[44] In this respect, the anionic mobility of the glasses obtained should be examined.

^{19}F and ^{27}Al NMR. The ^{19}F MAS NMR spectra of the $0.75K_2NbOF_5$−$0.25AlF_3$ glass and the initial $K_2NbOF_5 \cdot H_2O$ are shown in Figure 4. A static ^{19}F NMR spectrum of the latter

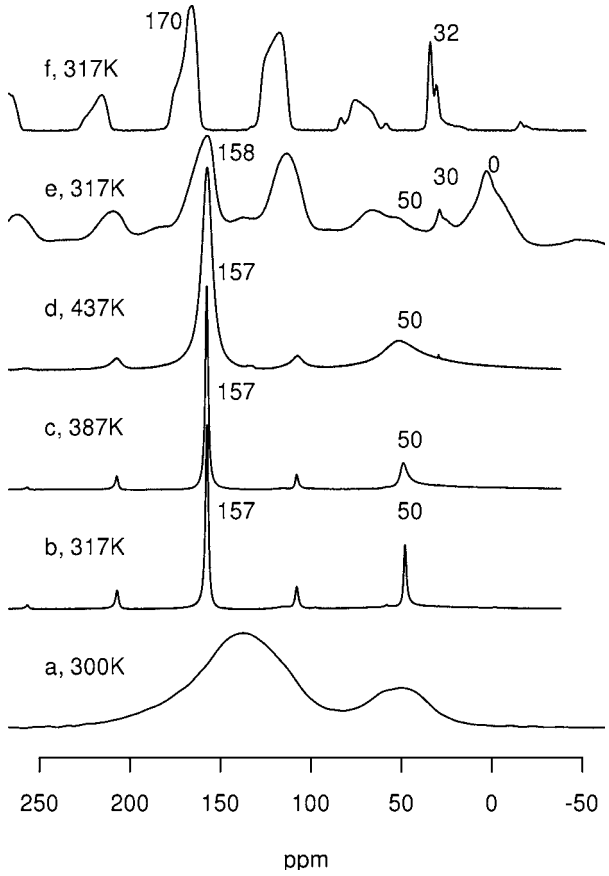

Figure 4. Static (a) and MAS (b−f) ^{19}F NMR spectra of $K_2NbOF_5 \cdot H_2O$ (a−d), K_2NbOF_5−AlF_3 glass (e), and $K_3Nb_2O_2F_9 \cdot (KF)_{0.333}$ (f). Isotropic CS values are shown near the peaks, and spinning sidebands are left unmarked.

is also presented (Figure 4a). The ^{19}F MAS NMR spectra of $K_2NbOF_5 \cdot H_2O$ have perfect resolution at a rotational frequency of ≥12 kHz and consist of two peaks at 50 and 157 ppm. The integrated intensities of the peaks have a ratio of 1:4. Because this intensity ratio is the same as the multiplicity ratio of the axial to equatorial fluoride ions, the first one (F_a) appears at 50 ppm and the equatorial one (F_e) appears at 157 ppm. These CS peaks virtually coincide with those reported for dynamically disordered $(NH_4)_2NbOF_5$[45] and somewhat differ from those in ordered oxofluoroniobate with organic cations.[46]

dx.doi.org/10.1021/ic302395x | *Inorg. Chem.* 2013, 52, 5722−5728

At temperatures 400 K and higher, the line widths increase and their shape changes from the Gaussian to the Lorentzian. This spectral transformation can be explained by the onset of fluorine exchange in the $NbOF_5$ polyhedra between the two types of fluorine sites. The temperature limitation of the MAS probe did not allow us the observation of further spectral transformation and emergence of a single line of the averaged CS. This effect was observed on static spectra (Figure 5). It

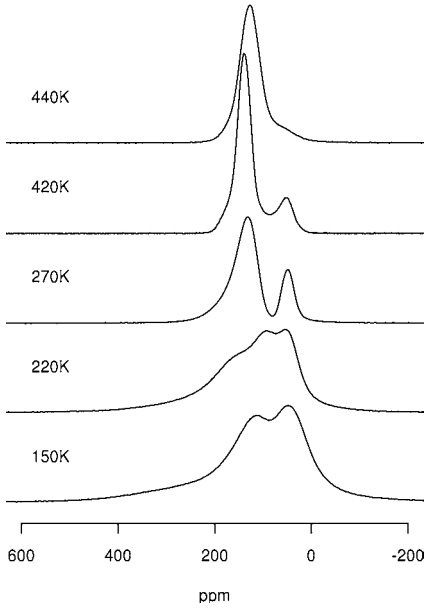

Figure 5. Temperature-dependent static ^{19}F NMR spectra of $K_2NbOF_5\ H_2O$.

should be noted that both single-pulse and Hahn echo spectral registration methods produce considerable line-shape distortions. The single-pulse spectra have extra peculiarities because of the loss of the initial part of free induction decay. Employment of the Hahn echo pulse sequence enabled us to overcome this problem, but the spectral shape is affected by the anisotropic fluorine diffusion. This should be taken into account during static and MAS spectral comparison.

At lower temperatures (below 240 K), the observed shape of the static ^{19}F NMR spectra (Figure 5) is determined by the structural nonequivalence of F atoms in the $NbOF_5$ octahedron and CS anisotropy. Above 270 K, the spectrum is described by two lines at a distance of ≈90 ppm that allow observation of a well-resolved two-component spectrum with an intensity ratio of ≈4:1 and CSs of 138 and 52 ppm attributed to F_e and F_a, respectively. The data obtained also confirm the absence of $F_e \leftrightarrow F_a$ exchange and intramolecular dynamics of the pseudorotation type (Bailar twist[47]) at 270−370 K.

The F_a CS (≈52 ppm) does not virtually change in the temperature range 150−420 K. Because these F atoms are characterized by the C_4 axial symmetry, they must comply with the equation $\delta_{11}([F]^-) = \delta_{22}([F]^-) = \delta_{\perp}([F]^-)$. The CS anisotropy of this component is insignificant, so all three main components of the second rank tensor are equal, and a line shape is determined mainly by dipole−dipole interaction of magnetic nuclei.

Another situation is observed in the case of the F_e component at lowering the temperature from 270 to 150 K. Below 220 K, the ^{19}F NMR spectrum is characterized by "fine" structure, which allows determination of the value of two components of the CS tensor, $\delta_{11}([F]^-)$ and $\delta_{22}([F]^-)$, corresponding to the magnetic field orientation perpendicular to the Nb−F bond. The value of the third component $\delta_{33}([F]^-)$ can be calculated from the formula for $\delta_{iso}([F]^-)$:

$$\delta_{iso}([F]^-) = \frac{1}{3}[\delta_{11}([F]^-) + \delta_{22}([F]^-) + \delta_{33}([F]^-)] \quad (1)$$

Inequality of $\delta_{11}([F]^-)$ and $\delta_{22}([F]^-)$ is evidence of nonaxial Nb−F chemical bonds that are described by the asymmetry parameter of the CS tensor η:

$$\eta = [\delta_{11}([F]^-) - \delta_{22}([F]^-)]/[\delta_{iso}([F]^-) - \delta_{33}([F]^-)] \quad (2)$$

Above 440 K, the spectrum transforms into a single line with the CS of 120 ppm, the width of which decreases with increasing temperature. It should be noted that the line position corresponds to the center of gravity of the two-component spectrum, $\langle\delta\rangle = (1/5)(4 \times 138 + 52) \approx 121$ ppm. This means that the fast $F_e \leftrightarrow F_a$ intramolecular exchange takes place at higher temperatures. Note that a similar situation occurs at temperatures above 340 K in $(NH_4)_3NbOF_6$;[45] the data obtained indicate a certain nonrigidity of the $[NbOF_6]^{3-}$ polyhedron with the $F_e \leftrightarrow F_a$ intramolecular dynamics when the local symmetry changes from C_{2v} to C_{5v}.

The spectral lines of ^{19}F MAS NMR of the glass studied (Figure 4e) are noticeably wider than those of the polycrystalline model compound $K_2NbOF_5{\cdot}H_2O$, which is explained by a range of interatomic distances and angles in the glass and significant (3.5 kHz) J coupling with 100% abundant ^{93}Nb atom[46] characterized by strong nuclear quadruple and magnetic moments ($I = {}^9/_2$). The signal assignment performed on the model compound makes the analysis of the glass spectra straightforward. The peak at 158 ppm has virtually the same CS as equatorial F atoms in the model compound. Therefore, it can be concluded that a significant part of these F atoms do not virtually participate in the formation of a glass network remaining as terminal. On the other hand, the 50 ppm line corresponding to the axial F atom is much less intensive; i.e., this F atom becomes bridging in the glass structure, and its CS must fall in the lower frequency range. Our preliminary quantum-mechanical calculations of the $Nb_2O_2F_9^{3-}$ dimer with the bridging F atom have shown that the CS of this atom should have a value close to that of the axial F atom in isolated $NbOF_5^{2-}$. Thus, a peak at 30 ppm belongs, probably, to bridging F atoms. The ^{19}F MAS NMR spectrum of $K_3Nb_2O_2F_9{\cdot}(KF)_{0.333}$ (Figure 4f) consisting of $Nb_2O_2F_9^{3-}$ dimers with the bridging F atom[48] corroborates our assignment. The peak at 32 ppm indicates that the bridging F atom joins two niobium octahedra, so the line at 30 ppm must be assigned to the bridging −Nb−F−Nb− fragment in glass chains.

Although the peak near 100 ppm has almost the same intensity as that at 157 ppm, its position is dependent on the MAS rotation speed and, therefore, it belongs to the spinning sideband.

A broad complex line around 0 ppm can be assigned to Al−F terminal and Al−F−Al structural units with the Al atom in octahedral coordination.[49] The ^{27}Al MAS spectrum (not shown) exhibits a single resonance at −5 ppm that corroborates its octahedral surroundings.[50]

The same spectral components affected by the CS anisotropy can be seen in the static spectra of the K_2NbOF_5−AlF_3 glass (Figure 6). Variable-temperature ^{19}F NMR measurements show

dx.doi.org/10.1021/ic302395x | Inorg. Chem. 2013, 52, 5722−5728

that the spectral fragments of both $NbOF_5$ and AlF_6 groups are temperature-dependent.

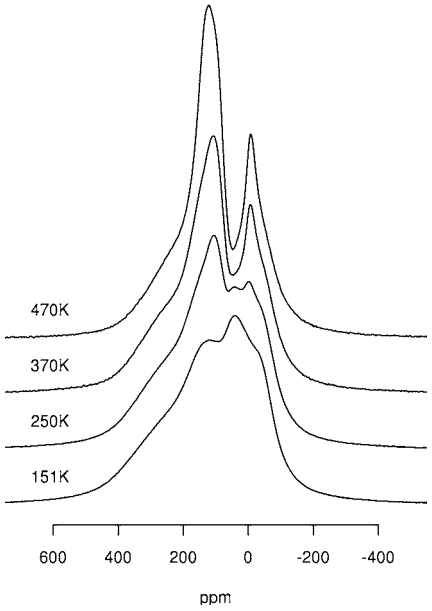

Figure 6. Temperature-dependent static ^{19}F NMR spectra of K_2NbOF_5–AlF_3 glass.

The character of the temperature transformations allows the statement that the corresponding complex anions ($NbOF_5$ and AlF_6) undergo molecular reorientations. Interestingly, the anionic motion in $Ba_5Al_3F_{19}$, consisting of isolated and chains of AlF_6^{3-} octahedra, includes a fast reorientation of isolated AlF_6^{3-} and a slower chemical exchange involving bond breaking and re-formation.[51] Similar motions can be expected to be more pronounced in the glass.

Mechanism of Glass Formation. In accordance with Poeppelmeier et al.'s concept, the $NbOF_5^{2-}$ anion exhibits its trans-directing properties in constructing solids.[25−30] The most negatively charged oxide and *trans*-fluoride ligands are the most nucleophilic and reactive, so that coordination is preferential to those sites. In the melt state, the monomeric $NbOF_5^{2-}$ is the dominant species at ratios of O/Nb of around 1.[52] No oxygen bridging takes place because bands between 600 and 800 cm^{-1} are absent in the Raman spectra of the melt. Solid AlF_3 is built up from AlF_6 octahedra sharing exclusively their corners with the formation of a 3D network.[53] Upon heating, the weaker (and longer) Al−F bonds are broken, creating undercoordinated Al bonds that are potential Lewis acid sites similar to undercoordinated Al ions that are always exposed at the surface of α-AlF_3 crystallites or nanoparticles.[54] These Al ions are coordinated to either four or five F ions. One should also mention that monomeric forms of complexes AlF_4^-, AlF_5^{2-}, and AlF_6^{3-} are present in sodium cryolite melts.[55] Low (four or five)-coordinated species are expected to act as the Lewis acid sites, which can readily respond to $NbOF_5^{2-}$ binding through the O and *trans*-F atoms, forming a chainlike cluster with corner-shared octahedra according to the nominal glass composition $K_{1.5}Nb_{0.75}Al_{0.25}O_{0.75}F_{4.5}$ (the ligand-to-metal ratio is 5.25). The bridging fragments are Al−F−Nb, Nb−O−Al, and Nb−F−Nb (Figure 7). The latter emerges because of an undercoordinated (unsaturated) Al ion as a scavenger of fluorine, so that the 5-fold Nb ion in a truncated octahedral geometry is bound to an adjacent Nb octahedron by bridging fluorine. The higher than 5 ratio of ligand-to-metal of the glass composition means that isolated octahedra (most likely, $NbOF_5^{2-}$) must be present. Two isolated $NbOF_5^{2-}$ octahedra must be combined with the presented (Figure 7) cluster to be close to the above glass composition ($K_8Al_2Nb_4O_4F_{26}\cdot 2K_2NbOF_5 = K_{12}(Al_2Nb_6)O_6F_{36}$).

Taking into account fast reorientations of $NbOF_5^{2-}$octahedra (in accordance with the ^{19}F NMR data), one can assume that their jumping reorientations proceed so rapidly that the central atom does not keep pace with oxygen and remains near the symmetry center. In this case, Nb−O and Nb−F should be equalized (~1.9 Å). The calculation of this state results in synchronous vibrations of the Nb−O and Nb−F bonds, whose highest frequency falls above 700 cm^{-1}. This state of the polyhedron is not energy-minimized similarly to that described for $TaOF_5^{2-}$ (cluster $Rb_3TaOF_5^+$ was considered).[56] The calculations show that this vibration is both IR- and Raman-active. In fact, it appears only in the IR spectra. This spectral feature has also been mentioned for oxofluoroniobates in Flinak.[52a] This feature is much more pronounced in the Cu(Mn)$NbOF_5$-based glasses,[10−16] which must consist of alternating M^{2+} and Nb^{5+} octahedra (pyrochlore-like type structure). The addition of $Ba(Pb)F_2$ leads to a higher concentration of rapidly reoriented, isolated $NbOF_5$ octahedra.

CONCLUSIONS

The combined application of vibrational (IR and Raman) and solid-state NMR spectroscopy demonstrates a greater validity to resolve the rather complex short- and medium-range order of mixed network former glasses in the glass system K_2NbOF_5–AlF_3. The glass structure can be viewed as a collection of interlinked Nb and Al octahedral units, with the preference to geteroatomic linkages. The presence of tetrahedrally coordinated Al ions suggested[4] for this system was not confirmed. Disorder packing of corner-sharing or edge-sharing $NbOF_5$

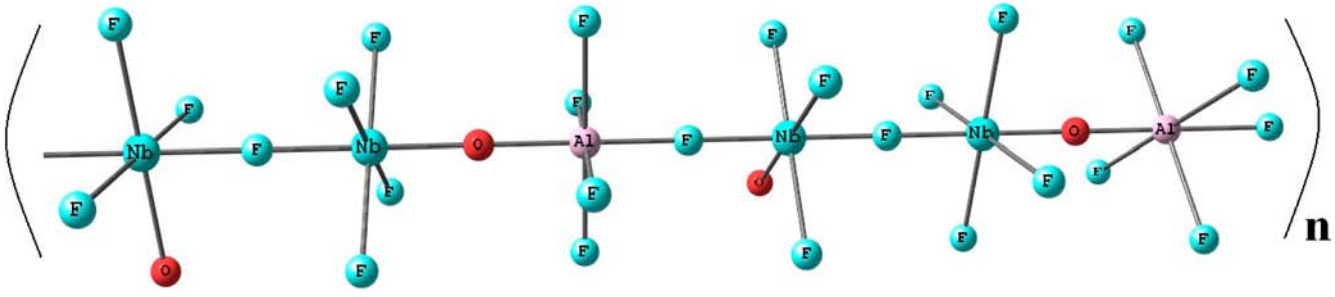

Figure 7. Chainlike fragment of the $K_{1.5}Nb_{0.75}Al_{0.25}O_{0.75}F_{4.5}$ glass.

dx.doi.org/10.1021/ic302395x | Inorg. Chem. 2013, 52, 5722−5728

octahedra in the LiF−$BaNbOF_5$ binary glass system[5] is also doubtful. The heteroatomic connectivities (Al−F−Nb and Nb−O−Al) are favored over homoatomic Nb−F−Nb linkages. The medium-range order of this glass system incorporates isolated $NbOF_5$ octahedra as well. During their fast reorientations, the central atom can remain near the octahedral center, so that the Nb−O and Nb−F distances are equalized, which results in the emergence of synchronous Nb−O and Nb−F stretches. The theoretical calculations show that these vibrations are both IR- and Raman-active. In fact, analysis of the literature data and our observations reveals that they are detected only in the IR spectra and are absent in the Raman spectra. This intriguing phenomenon calls for further investigations. However, this peculiarity can be used to distinguish isolated polyhedra from the bridging −M−O−M− species shown in both IR and Raman spectra. Thus, the assumption that the network of oxofluoroniobate glasses consists of chains of O-bridging niobium octahedra[10−16] is not proven.

■ ASSOCIATED CONTENT

Supporting Information

Tables S1−S3 containing powder XRD patterns (experimental and calculated) of triclinic and monoclinic modifications of $K_2NbOF_5{\cdot}nH_2O$ and $NaNbOF_4$ and Figure S1 showing TGA of triclinic $K_2NbOF_5{\cdot}nH_2O$ (n = 0.75) in quasi-isobaric conditions (labyrinth Pt crucible). This material is available free of charge via the Internet at http://pubs.acs.org.

■ AUTHOR INFORMATION

Corresponding Author

*E-mail: laptash@ich.dvo.ru. Fax: +7-423-2312590.

Author Contributions

The manuscript was written through contributions of all authors. All authors have given approval to the final version of the manuscript.

Notes

The authors declare no competing financial interest.

■ ACKNOWLEDGMENTS

Dr. T. B. Emelina is acknowledged for DFT calculations. We thank Drs. A. A. Udovenko and T. A. Kaidalova for identification of $K_2NbOF_5{\cdot}nH_2O$ and $NaNbOF_4$ and Dr. E. B. Merkulov for thermal curves of $K_2NbOF_5{\cdot}nH_2O$. The Russian Foundation for Basic Research (RFBR; Grant 11-03-00229) is acknowledged for financial support.

■ REFERENCES

(1) Nazabal, V.; Poulain, M.; Olivier, M.; Pirasteh, P.; Camy, P.; Doualan, J.-L.; Guy, S.; Djouama, T.; Boutarfaia, A.; Adam, J. L. *J. Fluorine Chem.* **2012**, *134*, 18−23.
(2) Polyshchuk, S. A.; Ignat'eva, L. N.; Marchenko, Yu. V.; Bouznik, V. M. *Glass Phys. Chem.* **2011**, *37*, 1−20.
(3) Hager, I. Z. *Mater. Chem. Phys.* **2008**, *109*, 365−372.
(4) Cui, H.; Yuan, Q. H.; Cui, W. Q. *J. Non-Cryst. Solids* **1989**, *107*, 219−224.
(5) Zhang, L. P.; Ye, A. M.; Feng, J. T.; Gan, F. X. *J. Non-Cryst. Solids* **1992**, *140*, 220−224.
(6) Klouche Bouchaour, Z. C.; Poulain, M.; Belhadji, M.; Hager, I.; El-Mallawany, R. *J. Non-Cryst. Solids* **2005**, *351*, 818−825.
(7) Ignat'eva, L. N.; Antokhina, T. F.; Polyshchuk, S. A.; Savchenko, N. N.; Bouznik, V. M. *Glass Phys. Chem.* **1998**, *24*, 97−100.
(8) Ignatieva, L. N.; Bouznik, V. M. *J. Non-Cryst. Solids* **1999**, *258*, 131−139.
(9) Ignat'eva, L. N.; Bouznik, V. M. *Russ. J. Struct. Chem.* **2000**, *41*, 212−216.
(10) Ignat'eva, L. N.; Polyshchuk, S. A.; Antokhina, T. F.; Zakalyukin, R. M.; Savchenko, N. N.; Kuryavyi, V. G.; Bouznik, V. M. *Russ. J. Inorg. Chem.* **2004**, *49*, 1651−1656.
(11) Ignat'eva, L. N.; Polyshchuk, S. A.; Antokhina, T. F.; Savchenko, N. N.; Bouznik, V. M. *Russ. J. Inorg. Chem.* **2005**, *50*, 12−14.
(12) Ignat'eva, L. N.; Polyshchuk, S. A.; Antokhina, T. F.; Bouznik, V. M. *Glass Phys. Chem.* **2005**, *46*, 153−156.
(13) Ignat'eva, L. N.; Antokhina, T. F.; Merkulov, E. B.; Polyshchuk, S. A.; Savchenko, N. N.; Plotnichenko, V. G.; Kaltashev, V. V.; Bouznik, V. M. *Russ. J. Inorg. Chem.* **2006**, *51*, 1532−1537.
(14) Ignat'eva, L. N.; Antokhina, T. F.; Polyshchuk, S. A.; Savchenko, N. N.; Merkulov, E. B.; Bouznik, V. M. *Russ. J. Inorg. Chem.* **2007**, *52*, 1328−1332.
(15) Ignat'eva, L. N.; Savchenko, N. N.; Surovtsev, N. V.; Antokhina, T. F.; Polyshchuk, S. A.; Marchenko, Yu. V.; Merkulov, E. B.; Bouznik, V. M. *Russ. J. Inorg. Chem.* **2010**, *55*, 925−931.
(16) Ignatieva, L. N.; Surovtsev, N. V.; Savchenko, N. N.; Adichtchev, S. V.; Polyshchuk, S. A.; Marchenko, Yu. V.; Bouznik, V. M. *J. Non-Cryst. Solids* **2011**, *357*, 3807−3812.
(17) Gabuda, S. P.; Gagarinsky, Yu. V.; Polyshchuk, S. A. *NMR in Inorganic Fluorides*; Atomic Energy Press (Atomizdat): Moscow, 1978; in Russian.
(18) Surendra, I.; Sathyanarayana, D. N.; Jere, G. V. *J. Fluorine Chem.* **1983**, *23*, 115−122.
(19) Pausewang, G.; Schmitt, R.; Dehnicke, K. *Z. Anorg. Allg. Chem.* **1974**, *408*, 1−8.
(20) Keller, O. L., Jr. *Inorg. Chem.* **1963**, *2*, 783−787.
(21) Mayer, J. M. *Inorg. Chem.* **1988**, *27*, 3899−3903.
(22) Sarin, V. A.; Dudarev, V. Ya.; Fykin, L. E.; Gorbunova, Yu. E.; Ilyin, E. G.; Buslaev, Yu. A. *Dokl. Akad. Nauk SSSR* **1977**, *236*, 393−396.
(23) Stomberg, R. *Acta Chem. Scand.* **1984**, *A 38*, 603−607.
(24) Halasyamani, P.; Willis, M. J.; Stern, C. L.; Lundquist, P. M.; Wong, J. K.; Poeppelmeier, K. R. *Inorg. Chem.* **1996**, *35*, 1367−1371.
(25) Heier, K. R.; Norquist, A. J.; Wilson, C. G.; Stern, C. L.; Poeppelmeier, K. R. *Inorg. Chem.* **1998**, *37*, 76−80.
(26) Norquist, A. J.; Heier, K. R.; Stern, C. L.; Poeppelmeier, K. R. *Inorg. Chem.* **1998**, *37*, 6495−6501.
(27) Norquist, A. J.; Stern, C. L.; Poeppelmeier, K. R. *Inorg. Chem.* **1999**, *38*, 3448−3449.
(28) Welk, M. E.; Norquist, A. J.; Arnold, F. P.; Stern, C. L.; Poeppelmeier, K. R. *Inorg. Chem.* **2002**, *41*, 5119−5125.
(29) Izumi, H. K.; Kirsh, J. E.; Stern, C. L.; Poeppelmeier, K. R. *Inorg. Chem.* **2005**, *44*, 884−895.
(30) Marvel, M. R.; Lesage, J.; Baek, J.; Halasayamani, P. S.; Stern, C. L.; Poeppelmeier, K. R. *J. Am. Chem. Soc.* **2007**, *129*, 13963−13969.
(31) Marvel, M. R.; Pinlac, R. A. F.; Stern, C. L.; Poeppelmeier, K. R. *Z. Anorg. Allg. Chem.* **2009**, *635*, 869−877.
(32) Feng, Y. Q.; Meng, Z. H.; Huang, Q. Z.; Qiu, D. F.; Shi, H. Z. *Inorg. Chem. Commun.* **2010**, *13*, 1118−1121.
(33) Pinsker, G. Z. *Kristallografiya* **1966**, *11*, 741−748.
(34) Udovenko, A. A.; Laptash, N. M. *Acta Crystallogr.* **2008**, *B64*, 527−533.
(35) Konig, R.; Scholz, G.; Scheurell, K.; Heidemann, D.; Buchem, I.; Unger, W. E. S.; Kemnitz, E. *J. Fluorine Chem.* **2010**, *131*, 91−97.
(36) Agulyansky, A. I. *The Chemistry of of Tantalum and Niobium Fluoride Compounds*; Elsevier: Amsterdam, The Netherlands, 2004.
(37) Lin, H.; Maggard, P. A. *Cryst. Growth Des.* **2010**, *10*, 1323−1331.
(38) Mattes, R.; Müller, G.; Becher, H. J. *Z. Anorg. Allg. Chem.* **1975**, *416*, 256−262.
(39) Patarin, J.; Marcuccilli-Hoffner, F.; Kessler, H.; Daniels, P. *Eur. J. Solid State Inorg. Chem.* **1994**, *31*, 501−511.
(40) Laptash, N. M.; Maslennikova, I. G.; Kaidalova, T. A. *J. Fluorine Chem.* **1999**, *99*, 133−137.

(41) (a) Sengupta, A. K.; Bhaumir, B. B. *Z. Anorg. Allg. Chem.* **1971**, *384*, 255−259. (b) Mattes, R.; Rieskamp, H. *Z. Naturforsch.* **1972**, *27 b*, 1421.
(42) Cordier, S.; Roisnel, T.; Poulain, M. *J. Solid State Chem.* **2004**, *177*, 3119−3126.
(43) Mattes, R.; Leimkuchler, M.; Nagel, A. *Z. Anorg. Allg. Chem.* **1990**, *582*, 131−142.
(44) Brink, F. J.; Withers, R. L.; Norén, L. *J. Solid State Chem.* **2002**, *166*, 73−80.
(45) Kavun, V. Ya.; Gabuda, S. P.; Kozlova, S. G.; Tkachenko, I. A.; Laptash, N. M. *J. Fluorine Chem.* **2011**, *132*, 698−702.
(46) Du, L. S.; Schurko, R. W.; Kim, N.; Grey, C. P. *J. Phys. Chem. A* **2002**, *106*, 7876−7886.
(47) Casanova, D.; Cirera, J.; Llunell, M.; Alemany, P.; Avnir, D.; Alvarez, S. *J. Am. Chem. Soc.* **2004**, *126*, 1755−1763.
(48) Udovenko, A. A.; Laptash, N. M. *Acta Crystallogr.* **2012**, *B68*, 602−609.
(49) (a) Kiczensky, T. J.; Stebbins, J. F. *J. Non-Cryst. Solids* **2002**, *306*, 160−168. (b) Body, M.; Legein, C.; Silly, G.; Buzaré, J.-Y. *J. Non-Cryst. Solids* **2007**, *353*, 2231−2236. (c) Martineau, C.; Legein, C.; Buzaré, J.-Y.; Fayon, F. *Phys. Chem. Chem. Phys.* **2009**, *11*, 950−957.
(50) Stosiek, C.; Scholz, G.; Schroeder, S. L. M.; Kemnitz, E. *Chem. Mater.* **2010**, *22*, 2347−2356.
(51) Martineau, C.; Fayon, F.; Suchomel, M. R.; Allix, M.; Massiot, D.; Taulelle, F. *Inorg. Chem.* **2011**, *50*, 2644−2653.
(52) (a) von Barner, J. H.; Christensen, E.; Bjerrum, N. J.; Gilbert, B. *Inorg. Chem.* **1991**, *30*, 561−566. (b) Andersen, K. B.; Christensen, E.; Berg, R. W.; Bjerrum, N. J.; von Barner, J. H. *Inorg. Chem.* **2000**, *39*, 3449−3454. (c) Vilk, A. F.; Dracopoulos, V.; Papatheodorou, G. N.; Østvold, T. *J. Alloys Compd.* **2001**, *321*, 284−299.
(53) Le Bail, A.; Calvayrac, F. *J. Solid State Chem.* **2006**, *179*, 3159−3166.
(54) (a) Chaudhuri, S.; Chupas, P.; Morgan, B. J.; Madden, P. A.; Grey, C. P. *Phys. Chem. Chem. Phys.* **2006**, *8*, 5045−5055. (b) Scholz, G.; König, R.; Petersen, J.; Angelow, B.; Dörfel, I.; Kemnitz, E. *Chem. Mater.* **2008**, *20*, 5406−5413. (c) Makarowicz, A.; Bailey, C. L.; Weiher, N.; Kemnitz, E.; Schroeder, S. L. M.; Mukhopadhyay, S.; Wander, A.; Searle, B. G.; Harrison, N. M. *Phys. Chem. Chem. Phys.* **2009**, *11*, 5664−5673. (d) Bailey, C. L.; Mukhopadhyay, S.; Wander, A.; Searle, B. G.; Harrison, N. M. *J. Phys. Chem. C* **2009**, *113*, 4976−4983.
(55) Nazmutdinov, R. R.; Zinkicheva, T. T.; Vassiliev, S. Yu.; Glukhov, D. V.; Tsirlina, G. A.; Probst, M. *Spectrochim. Acta, Part A* **2010**, *75*, 1244−1252.
(56) Laptash, N. M.; Udovenko, A. A.; Emelina, T. B. *J. Fluorine Chem.* **2011**, *132*, 1152−1158.